Optically detected electron paramagnetic resonance of Ni-related defects in synthetic diamond crystals

1998 J. Phys.: Condens. Matter 10 9833

(http://iopscience.iop.org/0953-8984/10/43/027)

J. Phys.: Condens. Matter **10** (1998) 9833–9840. Printed in the UK PII: S0953-8984(98)95083-4

Optically detected electron paramagnetic resonance of Ni-related defects in synthetic diamond crystals

Th Pawlik†, C Noble‡ and J-M Spaeth†

† Universität Paderborn, Fachbereich Physik, 33098 Paderborn, Germany

‡ Physics Department, Monash University, Clayton 3168, Australia

Received 15 June 1998, in final form 3 August 1998

Abstract. Synthetic diamond crystals grown using a solvent catalyst that contains Ni were studied by optical detection of electron paramagnetic resonance (ODEPR) using the magnetic circular dichroism of the optical absorption (MCDA). The MCDA spectra in the infrared spectral region consist of a derivative-like line at 1.06 eV, single sharp lines at 1.29 and 1.40 eV, a complex phonon-split band with the zero-phonon line (ZPL) at 1.69 eV and a derivative-like doublet structure superimposed at 1.72 eV. All of these optical absorptions were shown to originate from paramagnetic defects. Using ODEPR it was possible to unambiguously assign the 1.72 eV doublet to the NE4 centre and the 1.40 eV line to the NIRIM-2 centre. The defect responsible for the ZPL at 1.06 eV has the same symmetry as the NIRIM-2 centre with a slightly larger $g_{\|}$-value. The NE4 centre was assigned to substitutional Ni^{+} associated with a carbon vacancy in a nearest-neighbour position whereas the NIRIM-2 centre was assigned to interstitial Ni^{+} with a distortion along a [111] axis.

1. Introduction

Synthetically grown diamond crystals very often contain transition metal impurities. The source of the impurities is the growth environment. The transition metals Ni, Fe, Co are often used as catalysts. Of these, Ni and Co are believed to enter the diamond lattice in the form of dispersed atoms [1, 2].

Diamonds synthesized using a nickel catalyst show optical absorption lines at 1.22, 1.40, 1.883, 2.51 and 3.1 eV [3, 4]. In addition, these diamond crystals show electron paramagnetic resonance (EPR) spectra, which were tentatively assigned to Ni-related defects. By detecting isotope effects it was recently shown that Ni is responsible for the 1.40 eV line [5]. Until now, the correlation of optical spectra and paramagnetic resonance was achieved only indirectly by studying EPR and optical absorption spectra in diamonds grown with different nickel-containing catalysts or at different stages of annealing [6, 7]. In an effort to establish a more direct correlation we used the method of optical detection of electron paramagnetic resonance (ODEPR) via the magnetic circular dichroism of the optical absorption (MCDA). Since the MCDA signal is proportional to the population difference of the ground-state Zeeman levels, a microwave transition induced within these Zeeman levels decreases the MCDA signal (see, e.g., [8]). Thus, the optically detected EPR spectrum can be obtained by monitoring the MCDA over the desired magnetic field range while applying a microwave field of constant frequency. With this method an unambiguous assignment of optical absorptions to specific EPR spectra can be made and thus it is possible to model centres in a safer way than by monitoring simultaneous changes in EPR spectra and optical spectra due to annealing.

0953-8984/98/439833+08$19.50

2. Experimental procedure

The sample used in the investigation was a Ni-catalysed synthetic diamond, grown at the National Institute for Research in Inorganic Materials (NIRIM), Japan. The sample was grown by the temperature gradient method using a pure nickel solvent catalyst at around 1500 °C and a pressure of 6 GPa. It was then annealed at 1700 °C–1800 °C for several hours at about 7–9 GPa.

The diamond had then a colour ranging from a golden yellow to brown throughout the crystal indicating some inhomogeneity.

The sample was polished into a cube with the cube faces corresponding to [111], $[1\bar{1}0]$ and $[11\bar{2}]$ axes with all dimensions less than 2 mm. The plane of rotation of the magnetic field was a $\{11\bar{2}\}$ plane. $\boldsymbol{B}_0$ at zero degrees corresponds to $\boldsymbol{B}_0 \parallel [1\bar{1}0]$ and $\boldsymbol{B}_0$ at 90 degrees corresponds to $\boldsymbol{B}_0 \parallel [111]$.

The ODEPR experiments were carried out in a custom-built spectrometer operating in the K band (24.1 GHz). An Oxford He bath cryostat equipped with a 3.5 T superconducting magnet allowed optical and microwave access to the sample at temperatures $T \geqslant 1.5$ K. For K-band operation the sample was placed in a cylindrical microwave cavity with optical access. K-band microwaves were provided by a klystron source (900 mW). Operation in a second microwave band (V band, 72 GHz) was possible using a varactor-tuned and frequency-multiplied Gunn oscillator producing 150 mW at 72 GHz. In the latter case the microwave energy was applied to the sample by placing the open end of the V-band waveguide in front of a cryostat window. The lower microwave power in this set-up was not found to be critical for the investigation of the 1.69 eV band and the 1.72 eV doublet due to the long spin–lattice relaxation times of both defects. In addition, the higher magnetic field range provided a higher MCDA signal and a better separation of defects with similar g-matrices.

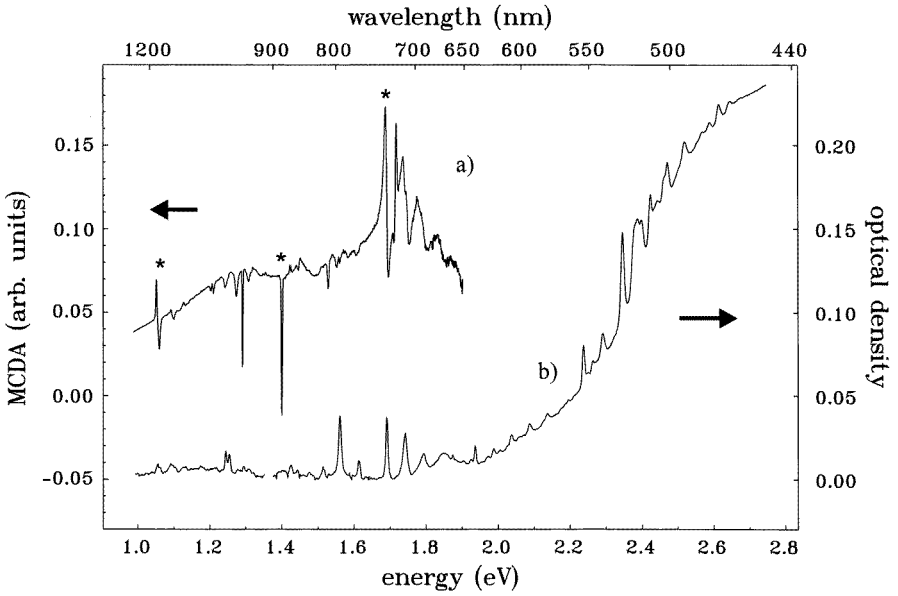

Figure 1. (a) The MCDA spectrum measured at $B = 2.5$ T, $T = 1.5$ K. (b) The optical absorption spectrum measured at $T = 1.5$ K.

In the case of the defects corresponding to the 1.06 and 1.40 eV lines, a much shorter spin–lattice relaxation time made the higher power of the K-band set-up necessary for the ODEPR measurements. The additional components for detecting the MCDA signal are described elsewhere [8]. The measurement temperature was 1.5 K or 4.2 K in all of the experiments.

3. Results and discussion

Figure 1, trace (a), shows an MCDA spectrum of the synthetic diamond measured at 1.5 K with $B = 2.5$ T. The corresponding optical absorption spectrum is shown as trace (b).

The optical absorption spectrum shows a number of sharp lines that have been previously reported [6] for Ni-catalysed diamonds in a similar annealing stage. The MCDA lines are temperature dependent. Their intensity decreases upon raising the temperature. This temperature dependence suggests that all of the bands in the MCDA spectrum originate from paramagnetic defects (see, e.g., [8]). Note that the doublet at 1.25 eV and the single line at 1.57 eV do not appear in the MCDA spectrum. It is therefore probable that these transitions belong to diamagnetic defects.

In a simple model of an atomic s $\rightarrow$ p transition, the appearance of either an absorption-shaped or a derivative-shaped MCDA depends on the magnitude of the spin–orbit splitting in the excited state versus the absorption bandwidth (see, e.g., [8]). For small spin–orbit splittings the MCDA lines are usually derivative whereas for large spin–orbit or crystal-field splittings one may observe separate bands for left- and right-circularly polarized light. The strong MCDA signal of the 1.40 eV and 1.29 eV lines compared to the rather small optical absorption suggests that these lines have a single circular polarization resulting in a strong dichroism of left- and right-circularly polarized light. The MCDA detection method using a modulated circular polarizer and lock-in amplifier leads to a very sensitive detection of the dichroism.

We have limited our ODEPR measurements to the study of the MCDA bands at 1.72 eV,

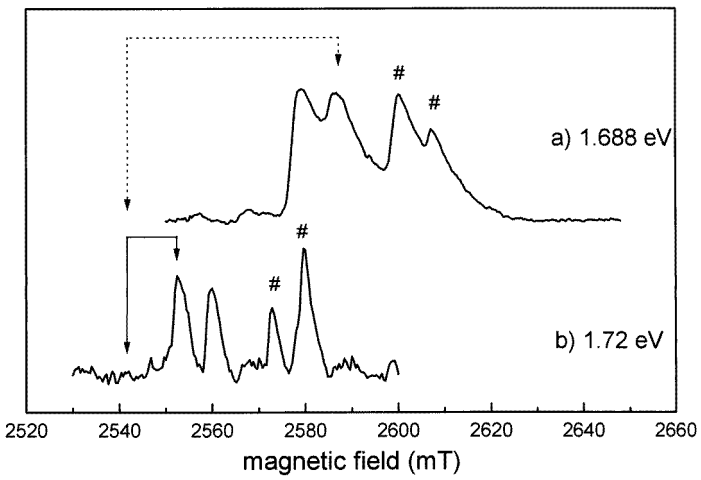

Figure 2. MCDA-detected EPR spectra measured at 1.688 eV (trace (a)) and 1.720 eV (trace (b)). The arrows indicate the magnetic field positions at which the MCDA spectra in figure 3 were measured. The microwave frequencies are 72.76 GHz and 73.32 GHz (see the text).

1.40 eV and 1.06 eV, marked by asterisks in figure 1, on trace (a). The band at 1.40 eV is of particular interest since it is found in the optical absorption spectrum of many synthetic diamonds. Conventional EPR studies [7, 9] have assigned different EPR spectra to this optical absorption band, mainly on the basis of the correlation of the EPR signal intensity and optical absorption spectra in a series of annealing experiments.

3.1. The 1.69 eV band and the 1.72 eV doublet

Figure 2 shows two MCDA-detected EPR spectra for $\boldsymbol{B} \parallel [111]$ measured at 1.688 eV (trace (a)) and 1.720 eV (trace (b)) with the V-band microwave source. Both EPR spectra exhibit four lines grouped into two doublets with a spacing of 20 mT between the two doublets. The appearance of two doublets has to be considered as an experimental artefact. It was found that the V-band microwave source produces, in addition to the fundamental frequency, a sideband which is 0.56 GHz higher in frequency and only 9 dB lower in power (this could be confirmed by measuring the MCDA-detected EPR of the well-studied F centres in KCl). Due to the long EPR spin–lattice relaxation times T_1, the low microwave power of the sideband is still sufficient to produce a significant change in the ground-state population and therefore an MCDA-detected EPR signal. The lines due to the second frequency at 73.32 GHz are marked by hash signs in figure 2. It will be shown later for the 1.720 eV MCDA that the internal splitting of the doublets is due to a slight misalignment of the crystal. This results in a splitting of the EPR lines corresponding to two orientations of the defect which would be degenerate for $\boldsymbol{B} \parallel [111]$.

From the results in figure 2 it is clear that the MCDA at around 1.7 eV is a superposition of MCDA spectra of at least two defects with different EPR spectra. In order to separate the two MCDA spectra we subtracted the MCDA spectrum with the magnetic field set on an EPR line from the MCDA spectrum measured at a nearby field position off the EPR line. The difference spectrum should only show the MCDA spectrum of the defect responsible for the EPR line. Due to the long spin–lattice relaxation time it was not possible to apply

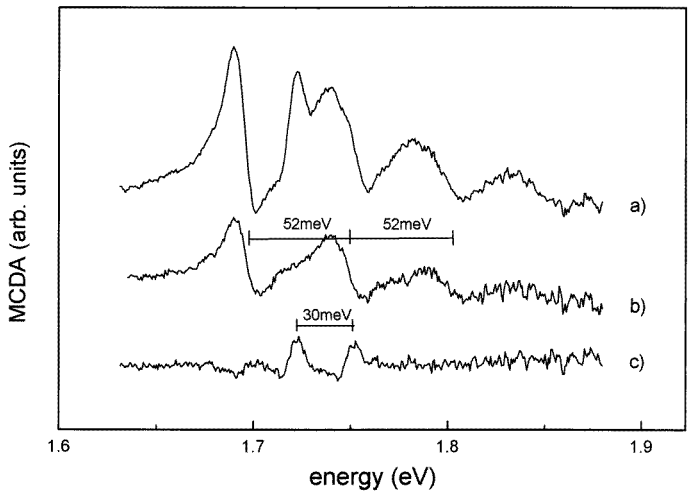

Figure 3. (a) The MCDA spectrum measured at $B = 2543$ mT, $T = 1.5$ K. (b) The difference of the MCDA spectra measured at 2543 mT and 2587 mT with an applied microwave field. (c) The difference of the MCDA spectra measured at 2543 mT and 2553 mT with an applied microwave field.

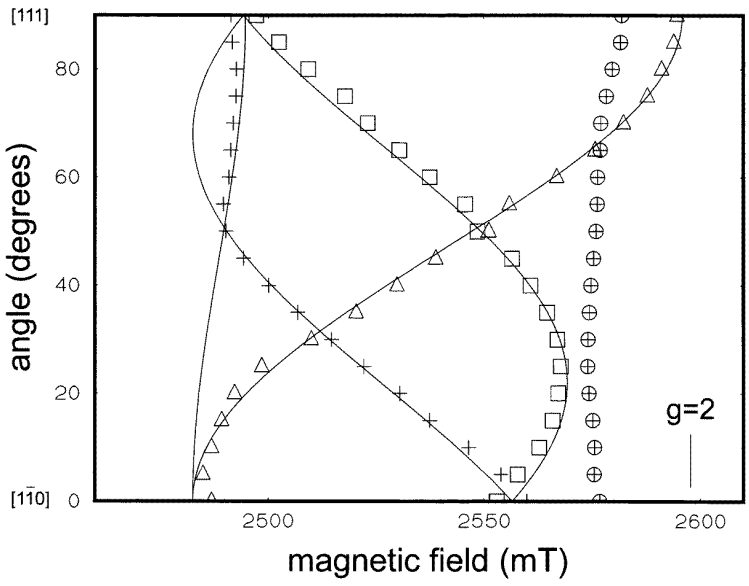

Figure 4. The ODEPR angular dependence of the defect responsible for the MCDA doublet at 1.72 eV and 1.75 eV. Zero degrees corresponds to $\boldsymbol{B} \parallel [1\bar{1}0]$. 90 degrees corresponds to $\boldsymbol{B} \parallel [111]$. The plane of rotation is a $\{11\bar{2}\}$ plane. The symbols represent the experimental EPR line positions. The solid lines are EPR line positions calculated using an axial g-matrix with the parameters $g_{\parallel} = 2.004 \pm 0.005$ and $g_{\perp} = 2.093 \pm 0.005$. The symbols $\oplus$ mark the positions of weak EPR lines from a nearly isotropic centre that was superimposed on the EPR spectrum of the 1.72/1.75 eV centre.

a microwave-modulation technique to measure the MCDA excitation spectrum of the EPR lines (see, e.g., [8]).

Figure 3 shows as trace (a) the MCDA spectrum obtained at $B = 2543$ mT. Trace (b) is the difference of the MCDA spectra measured at 2543 mT and 2587 mT (the two field positions are indicated by dotted arrows in figure 2). Trace (c) is the difference of the MCDA measured at 2543 mT and 2553 mT (marked by solid arrows in figure 2). The difference between traces (b) and (c) is apparent: trace (b) reproduces the phonon-split MCDA band with a ZPL at 1.688 eV and a phonon splitting of 52 meV. Trace (c), the MCDA responsible for the EPR spectrum given as trace (b) of figure 2, shows a doublet structure with a splitting of 30 meV.

The EPR angular dependence measured at 1.72 eV is shown in figure 4. The second resonance position due to the microwave sideband (marked by hash signs in figure 2) is not shown. The angular dependence can be explained well by assuming a defect with axial (111) symmetry and a g-matrix with the parameters $g_{\parallel} = 2.004 \pm 0.005$ and $g_{\perp} = 2.093 \pm 0.005$. These parameters are similar to the ones given in reference [7] for the NE4 centre ($g_{\parallel} = 2.023$ and $g_{\perp} = 2.098$, (111) symmetry). The defect was considered as a substitutional Ni^{+} ($3d^{9}$) defect associated with a C vacancy in a [111] direction. In reference [7], however, the authors assigned the EPR spectrum to the 1.40 eV absorption line. The difference in the values of $g_{\parallel}$ is somewhat larger than the experimental error. This difference could be due to the different measurement temperatures (EPR: 77 K; ODEPR: 1.5 K). However, the possibility that the EPR spectrum that we observed is a new Ni^{+} defect with a very similar structure to the NE4 centre cannot be ruled out.

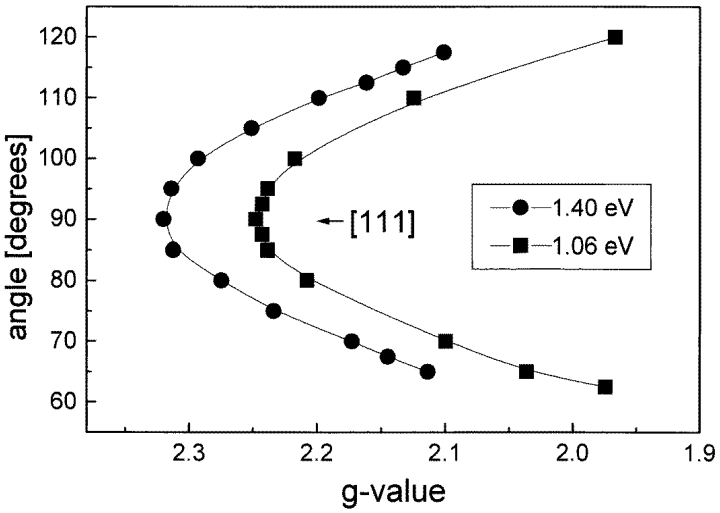

Figure 5. The ODEPR angular dependence of the defects responsible for the MCDA lines at 1.40 eV and 1.06 eV. 90 degrees corresponds to $\boldsymbol{B} \parallel [111]$. The plane of rotation is a $\{11\bar{2}\}$ plane.

3.2. 1.06 eV and 1.40 eV lines

Nazaré *et al* [1] have studied the fine structure of the 1.40 eV ZPL line in detail using high-resolution Zeeman spectroscopy. The authors found that a model of a paramagnetic $S = 1/2$ ground state with trigonal symmetry was able to explain the Zeeman shift within the ZPL fine structure. LCAO cluster calculations for Ni centres in various charge states and lattice positions were performed by Paslovsky and Lowther [10]. Isoya *et al* [9] have assigned the 1.40 eV optical transition to a defect detected in conventional EPR and labelled it NIRIM-2. The NIRIM-2 EPR centre is characterized by an axially symmetric g-matrix with $g_{\parallel} = 2.3285$ and $g_{\perp} \approx 0$ and (111) symmetry. With MCDA-detected EPR at 24.6 GHz, we found EPR signals in the MCDA at 1.40 eV when the crystal orientation was near a [111] direction. Figure 5 shows the angular dependence of the EPR measured in the MCDA at 1.40 eV (circles) and 1.06 eV (squares). The field axis was transformed to display g-values. Due to substantial line broadening, the angular dependence could not be followed for rotations $>20^{\circ}$ from the [111] axis. However, the apparent extrema at $\boldsymbol{B} \parallel [111]$ are consistent with a defect of (111) symmetry. The g-value ($g = 2.32 \pm 0.01$) measured at this angle is very close to the value of $g = 2.3285$ given for $g_{\parallel}$ in [9]. Therefore, the assignment of the 1.40 eV line to the NIRIM-2 EPR centre is very plausible. The angular dependence of the EPR measured in the 1.06 eV MCDA is similar, with the same axis of symmetry and a somewhat smaller $g_{\parallel}$ of 2.25.

Figure 6 shows in analogy to figure 3 the MCDA spectra responsible for the two different EPR centres. Trace (a) is the total MCDA spectrum. The inset shows the two EPR lines measured for $\boldsymbol{B} \parallel [111]$ in the MCDA transitions at 1.40 eV and 1.06 eV, respectively. The difference spectra given as traces (b) and (c) were obtained by subtracting the MCDA measured with microwave radiation at 750 mT and 774 mT from the MCDA measured at the same magnetic fields without microwave radiation. These spectra show that the absorption spectra of the EPR centres with $g_{\parallel} = 2.32$ and $g_{\parallel} = 2.25$ are indeed the 1.40 eV and 1.06 eV optical transitions, respectively.

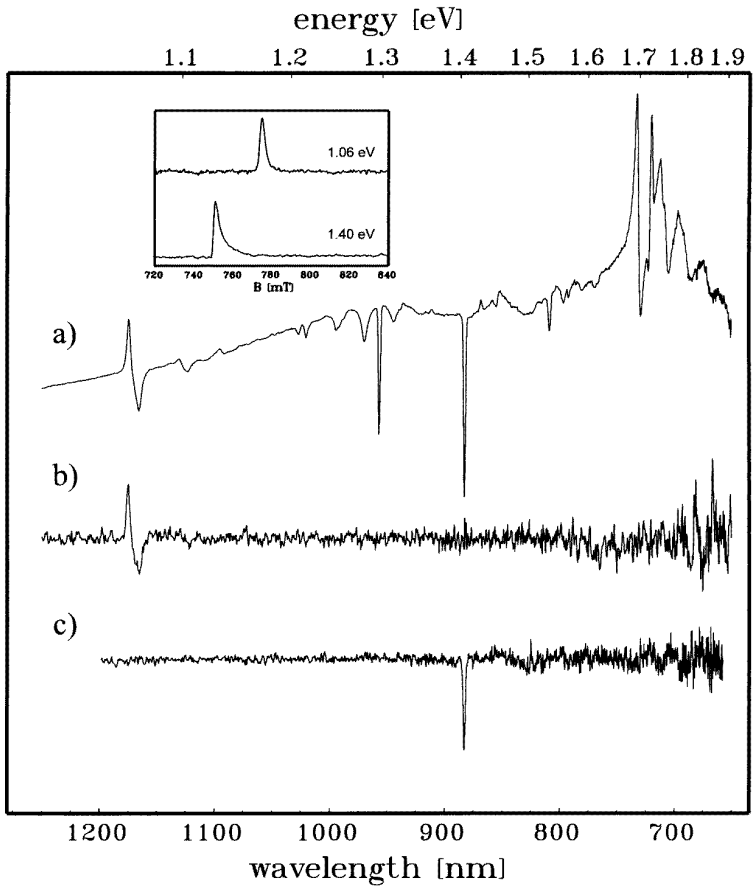

Figure 6. (a) The MCDA spectrum measured at $B = 2.5$ T, $T = 1.5$ K, $\boldsymbol{B} \parallel [111]$. (b) The difference of the MCDA spectra measured at $B = 750$ mT with and without microwaves. (c) The difference of the MCDA spectra measured at $B = 774$ mT with and without microwaves. Inset: MCDA-detected EPR spectra measured at 1.06 eV (upper spectrum) and 1.40 eV (lower spectrum).

4. Conclusions

We have shown that optical detection of electron paramagnetic resonance (ODEPR) via the magnetic circular dichroism of the optical absorption (MCDA) provides a direct correlation of optical absorptions and EPR spectra in diamonds. We have established a connection between the NE4 EPR centre and an absorption band at 1.72 eV as well as between the 1.40 eV line and the NIRIM-2 centre. A new EPR spectrum was detected in the MCDA at 1.06 eV. It has the same symmetry as the NIRIM-2 centre with a somewhat smaller $g_{\parallel}$-value. Further studies are needed to determine a structural model for this defect.

Acknowledgments

The authors would like to thank S C Lawson and H Kanda for the use of a Ni-catalysed synthetic diamond.

References

[1] Nazaré M H, Neves A J and Davies G 1991 *Phys. Rev.* B **43** 14 196
[2] Lawson S C, Kanda H, Watanabe K, Kiflawi I, Sato Y and Collins A T 1996 *J. Appl. Phys.* **79** 4348
[3] Collins A T, Kanda H and Burns R C 1990 *Phil. Mag.* B **61** 797
[4] Lawson S C, Kanda H and Sekita M 1993 *Phil. Mag.* B **68** 39
[5] Davies G, Neves A J and Nazaré M H 1989 *Europhys. Lett.* **9** 47
[6] Lawson S C and Kanda H 1993 *J. Appl. Phys.* **73** 3967
[7] Nadolinny V A and Yelisseyev A P 1993 *Diamond Relat. Mater.* **3** 1196
[8] Spaeth J-M, Niklas J R and Bartram R H 1992 *Structural Analysis of Point Defects in Solids: An Introduction to Multiple Magnetic Resonance Spectroscopy (Springer Series in Solid State Sciences 43)* (Berlin: Springer)
[9] Isoya J, Kanda H and Uchida Y 1990 *Phys. Rev.* B **42** 9843
[10] Paslovsky L and Lowther J E 1992 *J. Phys.: Condens. Matter* **4** 775